Journal of Imaging Science and Technology® 56(1): 010506-1–010506-9, 2012.

Simple Color Prediction Model Based on CIEXYZ Using an Effective Coverage Map

Yuanyuan Qu and Sasan Gooran
Department of Science and Technology, Linköping University, Campus Norrköping, Sweden
E-mail: qu.yuanyuan@liu.se

Abstract. *Most of the color prediction models use a single dot gain curve for each primary ink. In the proposed model, the behavior of the dot gain of each primary ink is characterized by three curves based on CIEXYZ tristimulus values. In our previous works, it was shown that the usage of three characterization curves for each primary ink reduced the color difference between the predicted and measured data compared with the simple Yule–Nielsen model. In this article, an effective coverage map based on CIEXYZ is created. This map presents the effective coverage values of the primary inks corresponding to different ink combinations. Given any reference ink combination, the effective coverage values of the involved primary inks are estimated by cubic interpolation. Compared to our previous models, the proposed model gives significant reduction in the color difference between the predicted and the measured data. © 2012 Society for Imaging Science and Technology.*
[DOI: 10.2352/J.ImagingSci.Technol.2012.56.1.010506]

INTRODUCTION

Most color prediction models share a common "lineage" to the original Murray–Davies (MD) model;[1] the most famous and almost the simplest model[2] is presented as the following equation:

$$R(\lambda) = aR_i(\lambda) + (1-a)R_p(\lambda), \tag{1}$$

where $R(\lambda)$ is the predicted spectral reflectance and a is the fractional area of the ink. $R_i(\lambda)$ is the spectral reflectance of the printed ink at full tone, and $R_p(\lambda)$ is the spectral reflectance of the substrate (usually paper). Because of the linear relationship between CIEXYZ values and the spectral reflectance, Eq. (1) can be extended to Eq. (2) based on CIEXYZ values, which is called Neugebauer's equations.[3]

$$\begin{bmatrix} X_{\text{ave}} \\ Y_{\text{ave}} \\ Z_{\text{ave}} \end{bmatrix} = \sum_i a_i \begin{bmatrix} X_i \\ Y_i \\ Z_i \end{bmatrix}, \tag{2}$$

where a_i is the fractional area covered by the ink or paper with CIEXYZ values (X_i, Y_i, Z_i) and $\sum_i a_i = 1$.

The coverage of each ink in Eq. (2) is supposed to be the physical coverage after print. However, aside from the physical dot gain, the optical dot gain also causes the print to be darker than the original bitmap. The optical dot gain is due to the scattering of light in the substrate,[4] lights that enter bare substrate might be scattered and exit from dot; lights that pass through a dot then might be scattered and exit from bare substrate. Hence, if there is only one ink involved, Eq. (2) can be rewritten as Eq. (3), which is used to deduce the effective coverage including both physical and optical dot gain of primary inks: cyan, magenta, yellow, and black (we only use cyan, magenta, and yellow).

$$\begin{bmatrix} X_{\text{ave}} \\ Y_{\text{ave}} \\ Z_{\text{ave}} \end{bmatrix} = a_i \begin{bmatrix} X_i \\ Y_i \\ Z_i \end{bmatrix} + (1-a_p) \begin{bmatrix} X_p \\ Y_p \\ Z_p \end{bmatrix}, \tag{3}$$

where (X_i, Y_i, Z_i) denote the CIEXYZ values of the full-tone ink (cyan, magenta, yellow) and (X_p, Y_p, Z_p) denote the CIEXYZ values of the paper. Equation (4) calculates the effective dot coverage based on CIEX for a certain amount of cyan.

$$ac_{\text{eff}} = \frac{Xc_{\text{mea}} - X_p}{X_c - X_p}, \tag{4}$$

where Xc_{mea}, X_c, and X_p denote the measured CIEX value of the halftone cyan, the full-tone cyan and the paper, respectively. ac_{eff} is the effective coverage of cyan for this patch. Since Eq. (4) has been carried out over a number of patches with different amount of only cyan, it gives a curve that illustrates the relationship between the effective and the reference coverage of cyan when it is printed on paper.

According to the experiments, the relationship between the reflectance spectra of a patch and the reflectance spectra of the involved full-tone ink as well as the white paper is actually not linear as assumed in Eq. (1). Yule and Nielsen's research on ink penetration and light scattering[5] showed the nonlinear relationship can be described with a power function

$$R^{1/n}(\lambda) = aR_i^{1/n}(\lambda) + (1-a)R_p^{1/n}(\lambda), \tag{5}$$

where n, which is referred to as the n-factor, is a parameter that accounts for light scattering in paper, while all the other variables have the same meaning as in Eq. (1). Fitting the n-factor requires nonlinear optimization.[1]

Received Sep. 23, 2011; accepted for publication Nov. 29, 2011; published online Mar. 14, 2012.
1062-3701/2012/56(1)/010506/9/$20.00.

Because of the nonlinear relationship in Eq. (5), the relationship between the CIEXYZ values of the patch and the CIEXYZ values of the involved full-tone ink and white paper is no longer linear as assumed in Eq. (3). However, Eq. (6), which is a modified version of Eq. (2), is commonly used to predict the CIEXYZ values of the average color using the *n*-factor.

$$\begin{bmatrix} X_{\text{ave}} \\ Y_{\text{ave}} \\ Z_{\text{ave}} \end{bmatrix}^{1/n} = \sum_i a_i \begin{bmatrix} X_i \\ Y_i \\ Z_i \end{bmatrix}^{1/n}. \tag{6}$$

Many prediction approaches have been discussed and examined in the literatures. Most of them are complicated, and some require nonlinear optimization. For example, point spread function or probability functions are used in the models to take into account the overall effect of light scattering;[6,7] Clapper–Yule model predicts the reflectance of the halftone prints by counting the multiple internal reflections between the print–air interface and the lateral light scattering within the paper bulk;[8] The Kubelka-Munk model approximates the light reflection by two light fluxes using light absorption and scattering coefficients;[9] Other ones include Yule–Nielsen modified spectral Neugebauer Model,[10] the improved Yule–Nielsen modified spectral Neugebauer model[11] and cellular Yule–Nielsen Neugebauer model[12,13] as well.

Most of the dot gain related models use single dot gain curve for each primary ink. Few researchers, for instance, in Refs. 10 and 11, applied different curves corresponding to different print situations, but still only one curve is obtained for each ink in a certain situation. When ink superposition happens, the dot gain of a certain amount of primary ink changes without obeying any observable rule. In this article, a simple model using characterization curves based on CIEXYZ tristimulus values will be presented.

The first step of our work was presented in Ref. 14. It indicates that using three characterized curves for each primary ink obtained by CIEX, Y, and Z, respectively, instead of a single curve, predicts the color values well when one or two primary inks are involved. The conclusion was supported by a comparison between our basic approach and the both MD and Yule–Nielsen (YN) models, by investigating the color difference between the predicted and the measured data. However, in the case of three inks involving, although the color differences between predicted and measured data were not satisfying, they were less than those obtained by the other two models. All the experiments were carried out using a laser printer and normal A4 office paper.

The work was followed by Ref. 15, in which the idea to take three curves based on CIEXYZ for each primary ink was kept and recarried out over the print samples using offset print device and coated paper with different halftone patterns. The color differences showed that our basic model works well for offset print device for almost all the halftone patterns we used, especially amplitude modulation (AM) and second generation frequency modulation with small dots (FM2-s).[15]

In Ref. 15, we tried to apply multiple dot gain curves based on CIEXYZ for each primary ink. They are the weighted sum of several possible curves. A possible curve based on CIEX for a primary ink, say, cyan, refers to the optimized dot gain curve using CIEX values when cyan is printed in possible situations, for example, on paper, or together with magenta, or together with both magenta and yellow, and so on. The weight for each possible curve is a kind of probability; it depends on the reference coverage of all the involved inks. That means the final three dot gain curves for each primary ink change as soon as any reference ink coverage varies.[15] The so-called multiple dot gain curves were more likely a kind of characterization curves for color calculation than the actual dot gain curves. Therefore, in the following text of this article, "characterization curve" is used instead of "dot gain curve".

Again, the obvious difference between the possible characterization curves for the same ink stood for the idea that only using one curve for each primary ink is not enough to correctly characterize the dot gain. The results in Ref. 15 showed that the usage of multiple characterization curves helps to decrease the ΔE_{94} color difference compared to the basic model proposed in Ref. 14. Unfortunately, the ΔE_{94} color differences were still beyond an acceptable level for the test laser printer, which is the same printer used in the present work.

As a continuation to those works, this article inherits two ideas: First, like in the basic model we characterize the behavior of the dot gain of each primary ink based on CIEXYZ tristimulus values; Second, the effective coverage values for a certain amount of primary ink are not always the same because of ink superposition. To execute the second idea, instead of multiple characterization curves, an effective coverage map is created in a simple way using several training patches. As soon as this map is created, given any ink combination, we just carry out cubic interpolation over the map to get the effective coverage of the involved primary inks.

THREE CHARACTERIZATION CURVES USING CIEXYZ

The three characterization curves mentioned above are denoted by dgc^X, dgc^Y, and dgc^Z in Eq. (7), in which cyan was taken as an example. The curves for magenta and yellow are obtained similarly.

$$\begin{aligned} c_{\text{eff}}^X &= \frac{Xc_{\text{mea}} - X_p}{X_c - X_p} = dgc^X + c_{\text{ref}}, \\ c_{\text{eff}}^Y &= \frac{Yc_{\text{mea}} - Y_p}{Y_c - Y_p} = dgc^Y + c_{\text{ref}}, \\ c_{\text{eff}}^Z &= \frac{Zc_{\text{mea}} - Z_p}{Z_c - Z_p} = dgc^Z + c_{\text{ref}}, \end{aligned} \tag{7}$$

where c_{eff}^X, c_{eff}^Y, and c_{eff}^Z are the effective dot coverage of cyan corresponding to the reference coverage value c_{ref}. X_p, Y_p,

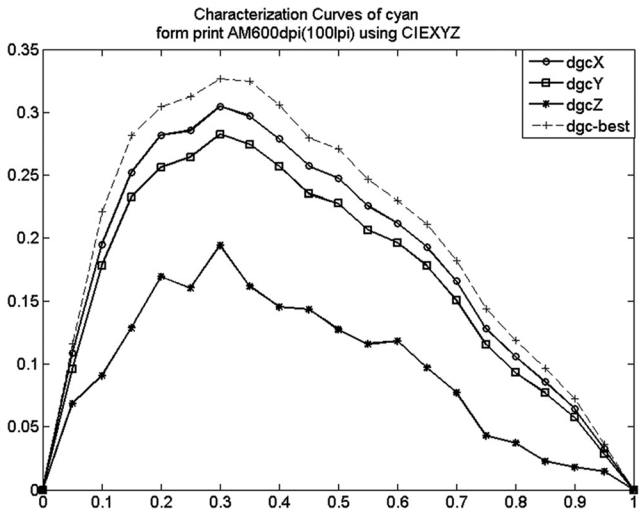

Figure 1. Characterization curves of cyan based on CIEXYZ printed by a laser printer (AM600 dpi_100 lpi).

and Z_p are CIEXYZ tristimulus value of paper, while X_c, Y_c, and Z_c are CIEXYZ tristimulus value of full-tone cyan. The measured CIEXYZ values of a halftone cyan patch are Xc_{mea}, Yc_{mea}, and Zc_{mea}. A group of cyan patches with percent coverage c_{ref} increasing from 0 to 100% enable us to get three characterization curves for cyan. The three characterization curves for magenta or yellow could be obtained similarly.

Figure 1 shows the three calculated characterization curves for cyan using AM600 dpi_100 lpi and printed by a laser printer (Xerox, Phaser 6180). The "best dot gain curve (or the best characterization curve)" in this figure which is denoted by *dgc-best* is an optimized curve obtained by first setting $dgc^X = dgc^Y = dgc^Z = dgc\text{-}best$ in Eq. (7). Then, the least square method was used to fix a series of coverage values giving the minimum ΔE_{Lab} color difference between measured and calculated data.

Since CIEXYZ tristimulus values have a linear relationship with the spectral reflectance, if the cyan ink and the paper are both ideal then it would only be possible to find the effective dot coverage for cyan by using the reflectance spectra in longer wavelength, which corresponds to CIEX values. Similarly, it would only be possible to find the effective dot coverage for magenta by using CIEY values and for yellow by using CIEZ values.[14] Fig. 1 clearly shows that the characterization curves of cyan using CIEX, CIEY, and CIEZ, respectively, differ from each other and from the "best dot gain curve." The similar situation occurs for magenta and yellow. Therefore, it is not completely correct to define only one characterization curve for each ink to be used in the Neugebauer's equations when calculating the resulting color values.

It should also be noticed that, in the measurement, there is actually optical dot gain included in the data. Hence, the calculated three effective coverage values for a certain amount of ink, in Eq. (7), include both the physical and optical dot gain. An advantageous proposal for color prediction is to use all the three different characterization curves based on CIEXYZ for each ink instead of a single curve. If the test patch only involves one ink, as soon as the ink's three characterization curves are created, the CIEXYZ tristimulus values of the test patch could be estimated by using the set of three effective ink coverage values obtained by interpolation along the three characterization curves.

When more than one primary ink is involved, Demichel's equations are used to get the fractional coverage over the patch using CIEX, Y, and Z for each primary and secondary colors. Equation (8) shows the fractional coverage for pure cyan, magenta, blue, and paper based on CIEXYZ when there are only cyan and magenta involved.

$$\begin{aligned}
&c^X = c^X_{\text{eff}} \bullet (1 - m^X_{\text{eff}}) \qquad c^Y = c^Y_{\text{eff}} \bullet (1 - m^Y_{\text{eff}}) \qquad c^Z = c^Z_{\text{eff}} \bullet (1 - m^Z_{\text{eff}}),\\
&m^X = m^X_{\text{eff}} \bullet (1 - c^X_{\text{eff}}) \qquad m^Y = m^Y_{\text{eff}} \bullet (1 - c^Y_{\text{eff}}) \qquad m^Z = m^Z_{\text{eff}} \bullet (1 - c^Z_{\text{eff}}),\\
&b^X = c^X_{\text{eff}} \bullet m^X_{\text{eff}} \qquad b^Y = c^Y_{\text{eff}} \bullet m^Y_{\text{eff}} \qquad b^Z = c^Z_{\text{eff}} \bullet m^Z_{\text{eff}},\\
&p^X = (1 - c^X_{\text{eff}}) \bullet (1 - m^X_{\text{eff}}) \quad p^Y = (1 - c^Y_{\text{eff}}) \bullet (1 - m^Y_{\text{eff}}) \quad p^Z = (1 - c^Z_{\text{eff}}) \bullet (1 - m^Z_{\text{eff}}).
\end{aligned} \tag{8}$$

The tristimulus values (X_{cal}, Y_{cal}, Z_{cal}) of the print could be calculated using Eq. (9) (take cyan accompanied with magenta as example). X_c, Y_c, and Z_c are the CIEXYZ values of full-tone cyan, the indices c, m, b, p refer to cyan, magenta, blue, and paper, respectively.

$$\begin{aligned}
X_{\text{cal}} &= c^X \bullet X_c + m^X \bullet X_m + b^X \bullet X_b + p^X \bullet X_p,\\
Y_{\text{cal}} &= c^Y \bullet Y_c + m^Y \bullet Y_m + b^Y \bullet Y_b + p^Y \bullet Y_p,\\
Z_{\text{cal}} &= c^Z \bullet Z_c + m^Z \bullet Z_m + b^Z \bullet Z_b + p^Z \bullet Z_p.
\end{aligned} \tag{9}$$

EFFECTIVE COVERAGE MAPPING

The proposed color prediction model predicts the color of the test patches with any CMY reference coverage values using several training patches. Therefore, we have to figure out the effective coverage of the primary inks for the training patches at the beginning. According to the experiments, the effective coverage of a certain amount of primary ink, say, cyan varies irregularly when there are different amount of magenta and yellow involved. In order to characterize the effective coverage of the inks in different combinations,

we chose [0, 25%, 50%, 75%, 100%] as the reference coverage for each ink. That means five training patches for each primary ink and totally 125 for different combinations of the primary inks.

The reference ink combination for each training patch contains three elements, which are the reference ink coverage value for cyan, magenta, and yellow, respectively. If we define a map in a coordinate system, whose three axes refer to the reference ink coverage of the three primary inks, the map then looks like a cubic box with 125 points located spatially uniform in the coordinate system; each point presents a training patch and its coordinates correspond to the three reference coverage values. The map is created by filling each point with three values corresponding to the three effective coverage values for each primary ink. During the mapping, the training patches involving one or two inks are treated differently from those with three inks.

In our model, training patches involving only one ink is treated the same way as patches with two inks where one of the effective coverage is set to zero. For the training patches involving only two inks, say, cyan and magenta, the effective coverage values should satisfy Eqs. (8) and (9). Equation (10) is the combination of Eqs. (8) and (9) if we take samples involving only cyan and magenta as example (For simplicity, we only focus on the equation based on CIEX).

$$\begin{aligned} c^X &= c^X_{\text{eff}} \bullet (1 - m^X_{\text{eff}}) \qquad & m^X &= m^X_{\text{eff}} \bullet (1 - c^X_{\text{eff}}), \\ b^X &= c^X_{\text{eff}} \bullet m^X_{\text{eff}} & p^X &= (1 - c^X_{\text{eff}}) \bullet (1 - m^X_{\text{eff}}), \\ X_{\text{mea}} &= c^X \bullet X_c + m^X \bullet X_m + b^X \bullet X_b + p^X \bullet X_p, \end{aligned} \tag{10}$$

where c^X_{eff} and m^X_{eff} are the wanted effective coverage for cyan and magenta based on CIEX; c^X, m^X, b^X, p^X are the fractional coverage of pure cyan, pure magenta, blue, and paper, respectively. X_{cal} in Eq. (9) is replaced by X_{mea} which refers to the real measured CIEX stimulus value. X_c, X_m, X_b, and X_p are the CIEX values of full-tone cyan, full-tone magenta, full-tone blue, and paper, respectively.

As X_{mea} is known by the measurement, there are two unknowns in Eq. (10): c^X_{eff} and m^X_{eff}. For prints with only one ink, for example, only 25% cyan, it is logical to set m^X_{eff} equal to 0 in Eq. (10). For prints with one halftone ink together with full tone of the other ink, for example, 25% cyan together with full-tone magenta, it is logical to set m^X_{eff} equal to 1 in Eq. (10). Then, for both examples the other unknown, which in this example is c^X_{eff}, could be obtained simply by solving Eq. (10).

In general cases, i.e., when none of the two unknowns are 0 or 1, there might be numerous pairs of values for c^X_{eff} and m^X_{eff} that satisfy Eq. (10). In the proposed model, the idea to fix an individual set of effective coverage values for the involved inks is explained as following.

Take the training patch ($c_{\text{ref}} = 0.5$, $m_{\text{ref}} = 0.25$) as an example, recall that c^X_{eff} refers to the effective coverage for cyan based on CIEX. Although c^X_{eff} (when $c_{\text{ref}} = 0.5$, $m_{\text{ref}} = 0.25$) differs from the c^X_{eff} (when $c_{\text{ref}} = 0.5$ and $m_{\text{ref}} \neq 0.25$), it should be close to c^X_{eff} (when $c_{\text{ref}} = 0.5$, $m_{\text{ref}} = 0$) and c^X_{eff} (when $c_{\text{ref}} = 0.5$, $m_{\text{ref}} = 0.5$) because they have the same reference coverage for cyan and they are two of the closest neighbors to the point ($c_{\text{ref}} = 0.5$, $m_{\text{ref}} = 0.25$) in the map. A point is a neighbor of another point if they have one reference coverage in common. Similarly, the effective coverage for 25% magenta m^X_{eff} (when $c_{\text{ref}} = 0.5$, $m_{\text{ref}} = 0.25$) differs from but should be close to the m^X_{eff} (when $c_{\text{ref}} = 0.25$, $m_{\text{ref}} = 0.25$) and (when $c_{\text{ref}} = 0.75$, $m_{\text{ref}} = 0.25$).

Figure 2 shows a 2D effective coverage grid for cyan and magenta. If we change cyan or magenta to yellow, except the measurement data, nothing else will change in the processing. For simplicity, we only focus on the effective coverage based on CIEX; the same process is carried out using CIEY and CIEZ values in the real execution of our approach. As discussed, the grid in Fig. 2 includes all the training patches that involve only cyan and magenta. The points on the borders (step 1, marked by star in Fig. 2) are actually the training patches with single ink or one halftone ink together with full tone of the other ink. As described before, the effective coverage of cyan and magenta for those points could be fixed simply because in these points the effective coverage of one of the inks is either 0 or 1. The points inside the grid are filled with the effective coverage values for each involved inks according to the values of their neighbors, see the example in the previous paragraph. The mapping then continues to fill the points on the corners of the inner-grid (step 2). Then, it fills the other points on the borders of the inner-grid (step 3) and finally fills the central point of the grid (step 4). A thorough description of how to do the mapping is given here.

Step 1. For the points marked by star on the borders of the grid, theoretically at least one of their two effective ink coverage is equal to 0 or 1. Therefore, the effective coverage of the other ink could be calculated easily using Eq. (10) as discussed before.

In the real operation, due to the possible measurement error or unstable printing, the calculated effective coverage value might be out of [0, 1]. The proposed model is tolerant to that but with the following limitations.

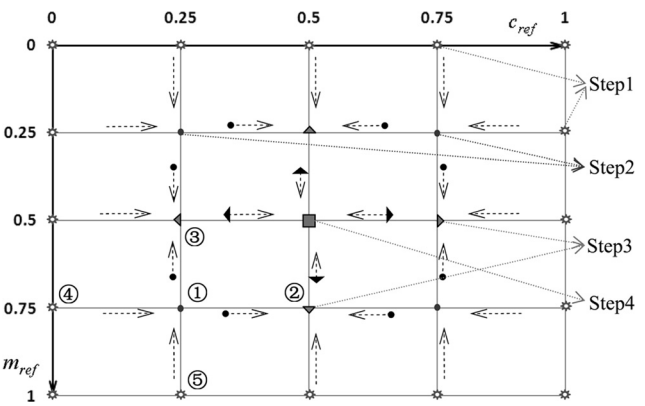

Figure 2. 2D effective coverage grid for the training patches with only cyan and magenta.

Effective coverage—reference coverage ≥ -0.2 and effective coverage ≤ 1.2. If the calculated values do not follow the limitations, we force them to obey the requirements at the expense of not satisfying Eq. (10). Once a set of effective coverage values have been found for a certain point, it is marked to show that it has already been filled.

Step 2. After step 1, the mapping goes to the points on the corners of the 3×3 inner-grid. These points, which are marked by dot in Fig. 2, have two neighbors that were filled previously in step 1. Recall that two points are neighbors if they are horizontally or vertically adjacent.

These two neighboring points might be located (up and left), (down and left), (up and right), (down and right) to the points in step 2, see Fig. 2. The effective coverage values of their already filled neighbors are used to limit the searching area within which we find a suitable pair of c_{eff}^X and m_{eff}^X that fit Eq. (10). Figure 3 is a framework to form a limited searching area for general cases, including all the points in steps 2–4. It runs when the point has at least two filled neighbors. Since we only focus on the procedures based on CIEX, c_{eff} and m_{eff} in Fig. 3 refer to c_{eff}^X and m_{eff}^X, respectively. All the four neighbors of a certain point are mentioned in Fig. 3, but not all of them will be considered to fix c_{eff}_max, c_{eff}_min, and m_{eff}_max, m_{eff}_min since some of these four might not have been filled yet. For example, in step 2, m_{eff}_right and c_{eff}_up are still unknown for point ($c_{\text{ref}} = 0.25$, $m_{\text{ref}} = 0.75$), which means (c_{eff}^1, m_{eff}^1) and (c_{eff}^2, m_{eff}^2) are unknown, then c_{eff}_max = max (c_{eff}^3, c_{eff}^4) replaces c_{eff}_max = max (c_{eff}^1, c_{eff}^2, c_{eff}^3, c_{eff}^4) in Fig. 3. Similar reasoning is also valid for c_{eff}_min, m_{eff}_max, and m_{eff}_min.

Let us give an example to explain how to fill the points in step 2. Take the point ($c_{\text{ref}} = 0.25$, $m_{\text{ref}} = 0.75$) as example, which is labeled with ① in Fig. 2. The effective coverage of 75% magenta m_{eff} ($c_{\text{ref}} = 0.25$, $m_{\text{ref}} = 0.75$) should be close to m_{eff}^1 and m_{eff}^3 in Fig. 3.

m_{eff}^1 is equal to m_{eff}_right, which is the value of m_{eff} for the right neighbor of point ①. The mentioned right neighboring point (labeled with ② in Fig. 2, $c_{\text{ref}} = 0.5$, $m_{\text{ref}} = 0.75$) has not been filled in the previous step; therefore, m_{eff}^1 is unknown;

m_{eff}^3 is equal to m_{eff}_left, which is the value of m_{eff} for the left neighbor of point ①. The mentioned left neighboring point (labeled with ④ in Fig. 2, $c_{\text{ref}} = 0$, $m_{\text{ref}} = 0.75$) is already filled in step 1 (assume that its value is 0.888), therefore $m_{\text{eff}}^3 = 0.888$.

Meanwhile, the effective coverage of 25% cyan c_{eff} ($c_{\text{ref}} = 0.25$, $m_{\text{ref}} = 0.75$) should be close to c_{eff}^2 and c_{eff}^4 in Fig. 3.

c_{eff}^2 is equal to c_{eff}_up, which is the value of c_{eff} for the up neighbor of point ①. The mentioned up neighboring point (labeled with ③ in Fig. 2, $c_{\text{ref}} = 0.25$, $m_{\text{ref}} = 0.5$) has not been filled in the previous step; therefore, c_{eff}^2 is unknown;

c_{eff}^4 is equal to c_{eff}_down, which is the value of c_{eff} for the down neighbor of point ①. The mentioned down neighboring point (labeled with ⑤ in Fig. 2, $c_{\text{ref}} = 0.25$, $m_{\text{ref}} = 1$) is already filled in step 1 (assume that its value is 0.413); Therefore $c_{\text{eff}}^4 = 0.413$.

Use Eq. (10) and X_{mea}, and set $c_{\text{eff}} = c_{\text{eff}}^4 = 0.413$ to get a value for m_{eff} which is $m_{\text{eff}}^4 = 0.869$. Similarly, we can get $c_{\text{eff}}^3 = 0.387$ when $m_{\text{eff}}^3 = 0.888$ is put in Eq. (10). Therefore, the searching area for c_{eff} ($c_{\text{ref}} = 0.25$, $m_{\text{ref}} = 0.75$) is from c_{eff}_min = 0.387 to c_{eff}_max = 0.413, and for m_{eff} ($c_{\text{ref}} = 0.25$, $m_{\text{ref}} = 0.75$) is from m_{eff}_min = 0.869 to m_{eff}_max = 0.888.

Within the limited searching area of effective coverage for cyan and magenta, we find those pairs of (c_{eff}, m_{eff}) that give calculated CIEX value with a maximum difference of 0.05 to the measured X_{mea}, see the text block for **Operation1** and **Operation2** below.

If there are several pairs that fit the requirement, see **Operation1**, we pick the pair that gives the minimum sum of the distances to (c_{eff}^i, m_{eff}^i) for $i = 1, 2, 3, 4$. In the above example, since there are many pairs which fit the requirement, the pair that gives the minimum sum of the distances to (c_{eff}^3, m_{eff}^3) and (c_{eff}^4, m_{eff}^4) is chosen. If there is no result fitting the requirement in the limited searching area, we enlarge or shift the searching area, see **Operation 2**.

Operation1

Limit $c_{\text{eff}} \in (c_{\text{eff}}\text{\_min}, c_{\text{eff}}\text{\_max})$; $m_{\text{eff}} \in (m_{\text{eff}}\text{\_min}, m_{\text{eff}}\text{\_max})$;

Within the limited area, find pairs of (c_{eff}, m_{eff}) that fit Eq. (10) with a tiny error of 0.05 allowed;

If there is no fits, within the limited area, pick the pair of (c_{eff}^*, m_{eff}^*) that produces the closest CIEX value to the measured CIEX, using Eq. (10). Then, do **Operation2**.

If there are several pairs that fit, pick the one which gives the minimum sum of the distances to (c_{eff}^1, m_{eff}^1), (c_{eff}^2, m_{eff}^2), (c_{eff}^3, m_{eff}^3) and (c_{eff}^4, m_{eff}^4); mark this point to show it is filled.

Operation2

Set $c_{\text{eff}} = c_{\text{eff}}^*$ in Eq. (10) and find out the value of the unknown element, i.e., m_{eff}. Denote it by m_{eff}^{**};

Set $m_{\text{eff}} = m_{\text{eff}}^*$ in Eq. (10) and find out the value of the unknown element, c_{eff}, this time; denote it by c_{eff}^{**}.

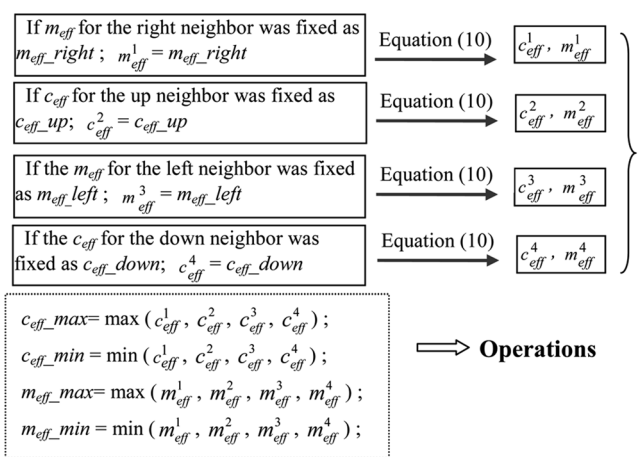

Figure 3. Reduce the searching area for suitable effective coverage for cyan and magenta. The c_{eff}^X and m_{eff}^X are written as c_{eff} and m_{eff}, respectively, for simplicity.

Now put $c_{\text{eff}}\_\min = \min\ (c^*_{\text{eff}},\ c^{**}_{\text{eff}})$; $c_{\text{eff}}\_\max = \max\ (c^*_{\text{eff}},\ c^{**}_{\text{eff}})$

$m_{\text{eff}}\_\min = \min\ (m^*_{\text{eff}},\ m^{**}_{\text{eff}})$; $m_{\text{eff}}\_\max = \max\ (m^*_{\text{eff}},\ m^{**}_{\text{eff}})$ and do **Operation 1**.

If **Operation2** goes more than five times without results, set c_{eff} = the latest c^*_{eff}; m_{eff} = the latest m^*_{eff}. **Mark** this point to show it is filled and go to the next point.

It should be noticed that $(c^i_{\text{eff}},\ m^i_{\text{eff}})$ for $i = 1, 2, 3, 4$ always satisfy Eq. (10), so they are obviously chosen during **Operation 1**. In order not to have equal effective coverage for two neighbors these pairs are excluded from the possible choices for $(c_{\text{eff}}, m_{\text{eff}})$ in **Operation 1**.

Step 3. The other four points on the borders of the inner-grid are marked by triangle in Fig. 2. These points have three neighbors that are already filled in steps 1 and 2. The same framework explained in Fig. 3 and Figure 4 are used to fill these points of the grid.

Step 4. The number of unfilled points continues to decrease and finally become the central point, whose four neighbors are filled in step 3. The same framework as for steps 1 and 2 is then used to fill this point.

Two other 2D effective coverage grids are similarly created for cyan-yellow and magenta-yellow. Given any reference ink coverage combination involving only two inks, the effective coverage values of the two primary inks could be obtained by cubic interpolation over those 2D effective coverage grids.

When it comes to the training patches involving three inks, the mapping will be slightly different. First, Eq. (10) is changed to Eq. (11) (here, we just show the equation using CIEX).

$$
\begin{aligned}
c^X &= c^X_{\text{eff}} \bullet (1 - m^X_{\text{eff}}) \bullet (1 - y^X_{\text{eff}}) \qquad m^X = m^X_{\text{eff}} \bullet (1 - c^X_{\text{eff}}) \bullet (1 - y^X_{\text{eff}}),\\
y^X &= y^X_{\text{eff}} \bullet (1 - m^X_{\text{eff}}) \bullet (1 - c^X_{\text{eff}}) \qquad r^X = m^X_{\text{eff}} \bullet y^X_{\text{eff}} \bullet (1 - c^X_{\text{eff}}),\\
g^X &= c^X_{\text{eff}} \bullet y^X_{\text{eff}} \bullet (1 - m^X_{\text{eff}}) \qquad b^X = c^X_{\text{eff}} \bullet m^X_{\text{eff}} \bullet (1 - y^X_{\text{eff}}),\\
k^X &= c^X_{\text{eff}} \bullet m^X_{\text{eff}} \bullet y^X_{\text{eff}} \qquad p^X = (1 - c^X_{\text{eff}}) \bullet (1 - m^X_{\text{eff}}) \bullet (1 - y^X_{\text{eff}}),\\
X_{\text{mea}} &= c^X \bullet X_c + m^X \bullet X_m + y^X \bullet X_y + r^X \bullet X_r + g^X \bullet X_g + b^X \bullet X_b + p^X \bullet X_p + k^X \bullet X_k,
\end{aligned}
\tag{11}
$$

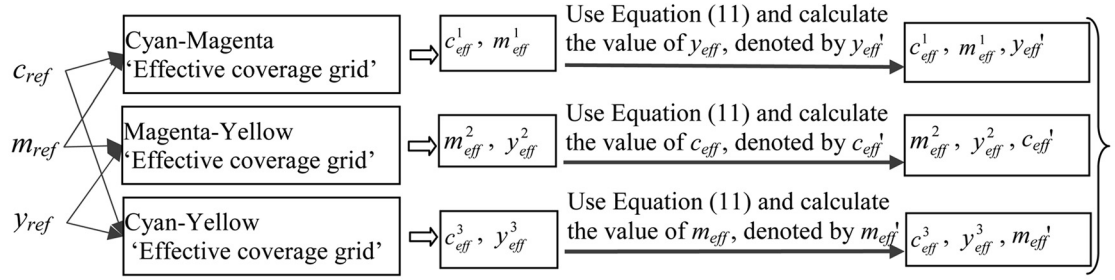

Operation1:

Limit $c_{eff} \in (\min(c^1_{eff}, c^3_{eff}),\ \max(c^1_{eff}, c^3_{eff}))$;

$m_{eff} \in (\min(m^1_{eff},\ m^2_{eff}), \max(m^1_{eff},\ m^2_{eff}))$;

$y_{eff} \in (\min(y^2_{eff},\ y^3_{eff}), \max(y^2_{eff},\ y^3_{eff}))$;

Within the limited area, find sets of (c_{eff}, m_{eff}, y_{eff}) that fit **Equation 11** with error less than (0.05).

If there is no fits within the limited area, then pick the set that produces the closest CIEX value to the measured CIEX, using Equation 11. Mark this set as (c_{eff}*, m_{eff}*, y_{eff}*). Then Do **Operation2**.

If there are several sets that fit, then pick the set that gives the minimum sum of the distances to $(c^1_{eff}, m^1_{eff}, y_{eff}')$, $(c_{eff}', m^2_{eff}, y^2_{eff})$ and $(c^3_{eff}, m_{eff}', y^3_{eff})$.

Operation2:

Set $c_{eff} = c_{eff}$*, $m_{eff} = m_{eff}$* in Equation (11), using X_{mea} which is the measured CIEX value of the training patch, find the value of y_{eff}, denote it by y_{eff}**.

Similarly set $(m_{eff}, y_{eff}) = (m_{eff}$*, y_{eff}*) to get c_{eff}**;

Similarly set $(c_{eff}, y_{eff}) = (c_{eff}$*, y_{eff}*) to get m_{eff}**;

Find the absolute value of following differences:

$|\ c_{eff}$*- c_{eff}** $|$, $|\ y_{eff}$*- y_{eff}** $|$ and

$|\ m_{eff}$*- m_{eff}** $|$, pick the one that has smallest value .

If c_{eff}* and c_{eff}** are the closest, then pick the set (c_{eff}**, m_{eff}*, y_{eff}*) to fill the corresponding point in the map.

If m_{eff}* and m_{eff}** are the closest, then pick the set (c_{eff}*, m_{eff}**, y_{eff}*) to fill the corresponding point in the map.

Or if y_{eff}* and y_{eff}** are the closest, then pick the set (c_{eff}*, m_{eff}*, y_{eff}**) to fill the corresponding point in the map.

Figure 4. Framework for creating the 3D effective coverage map. c^1_{eff} and m^1_{eff}, m^2_{eff} and y^2_{eff}, c^3_{eff} and y^3_{eff} are calculated by using the corresponding 2-D effective coverage grids.

where c_{eff}^X, m_{eff}^X, and y_{eff}^X are the wanted effective coverage based on CIEX for cyan, magenta, and yellow; c^X, m^X, y^X, r^X g^X, b^X, k^X, and p^X are the fractional coverage for pure cyan, magenta, yellow, red, green, blue, black, and paper, respectively. X_{mea} refers to the real measured CIEX stimulus value of a certain patch. X_c, X_m, X_y, X_r, X_g, X_b, X_k, and X_p are the CIEX values of each full-tone primary and secondary colors.

Second, the 2D effective coverage grids are used to set the limited searching area for involved primary inks. Fig. 4 shows how to fill the effective coverage map.

c_{eff}^1 and m_{eff}^1, m_{eff}^2 and y_{eff}^2, c_{eff}^3 and y_{eff}^3 are calculated by using the corresponding 2D effective coverage grids.

The same procedure has to be carried out to fill the points in the map with effective coverage values of each ink corresponding to CIEY and CIEZ, respectively.

When every single point in the map has been filled with the effective coverage values for three primary inks based on CIEXYZ, the 3D effective coverage map is built. Given any ink combination, the corresponding effective coverage based on CIEXYZ could be found by cubic interpolation over the map. Demichel's equations for three inks are then used to estimate the fractional coverage over each patch using CIEX, Y, and Z for each primary and secondary inks. The predicted color tristimulus values could finally be calculated using Eq. (12)

$$\begin{aligned} X_{\text{cal}} &= c^X \bullet X_c + m^X \bullet X_m + y^X \bullet X_y + r^X \bullet X_r + g^X \bullet X_g + b^X \bullet X_b + p^X \bullet X_p + k^X \bullet X_k, \\ Y_{\text{cal}} &= c^Y \bullet Y_c + m^Y \bullet Y_m + y^Y \bullet Y_y + r^Y \bullet Y_r + g^Y \bullet Y_g + b^Y \bullet Y_b + p^Y \bullet Y_p + k^Y \bullet Y_k, \\ Z_{\text{cal}} &= c^Z \bullet Z_c + m^Z \bullet Z_m + y^Z \bullet Z_y + r^Z \bullet Z_r + g^Z \bullet Z_g + b^Z \bullet Z_b + p^Z \bullet Z_p + k^Z \bullet Z_k. \end{aligned} \tag{12}$$

For training patches, which are also the points in the map, the effective coverage values of primary inks are constrained to fit Eq. (10) or Eq. (11). Hence, the color differences ΔE_{94} between the predicted and measured data are very small for those 125 training patches.

Notice that the Effective coverage map in this article is different from the cells in the cellular Yule–Nielsen Neugebauer model. The eight corners of a cell in the cellular Yule–Nielsen Neugebauer model illustrate the eight so-called sub-Neugebauer primaries which are chosen to replace the normal eight Neugebauer primaries (cyan, magenta, yellow, blue, red, green, and black) in the Yule–Nielsen Neugebauer equation. Furthermore, the cellular Yule–Nielsen Neugebauer model normalizes the ink coverage values of a certain sample according to the subdomain this sample belongs to. It does not characterize the effective coverage values for each ink according to reference ink combinations, which is actually what we have done and explained above.

RESULTS AND CONCLUSION

The proposed model is applied to a large number of color samples, consisting of 729 special patches with reference primary ink coverage picked from [0, 0.13, 0.25, 0.38, 0.5, 0.63, 0.75, 0.88, 1] and 519 patches with random reference primary ink coverage. A laser printer (Xerox, Phaser 6180) and uncoated A4 paper are used. The prints are divided into four groups using AM and first generation frequency modulated (FM1st) halftone pattern, the print resolution and screen frequency are 600 dpi (100 lpi) and 300 dpi (100 lpi) for AM and 300 dpi for FM1st. For the AM halftoning, we use circular dots and different screen anglers for cyan, magenta, and yellow (15° for cyan, 75° for magenta, and 0° for yellow). For FM halftoning, we use the method described in Ref. 16. The prints were measured by a spectrophotometer (BARBIERI electronic Spectro LFP RT) using D65 light source for a 2° observer.

The training patches are included in those 729 special patches mentioned above. As introduced in the "Effective Coverage Mapping" section, the reference coverage of training patches is picked from [0, 0.25, 0.5, 0.75, 1], which means a total of 125 training patches. It is flexible to choose [0, 0.25, 0.63, 0.88, 1] or [0, 0.25, 0.5, 0.75, 0.88, 1] instead of [0, 0.25, 0.5, 0.75, 1] as the reference coverage for the training patches. However, in this study, we use the medial series [0, 0.25, 0.5, 0.75, 1].

Another model, presented in Ref. 11, is also applied to help us to evaluate the performance of our proposed color prediction model. This model is an improved Yule–Nielsen modified spectral Neugebauer model using a special effective dot surface coverage computation model,[11] in which the effective coverage values are found by weighting the contributions from different reproduction curves according to the weights of the contributing superposition conditions. That model is operated based on spectrum reflectance, while our proposed model is only using CIEXYZ values. During the measurement, spectral data and CIEXYZ values are obtained at the same time. The color differences achieved by the two models are listed in Table I.

The *n*-factor used for improved Yule–Nielsen modified spectral Neugebauer model is optimized using 44 samples for each group each time and then is used for the other testing samples in that group. The spectrum data used in this model are recorded every 10 nm from 380 to 730 nm.

The color difference for the 1248 patches is divided into five teams: "Special (729)" refers to those 729 special patches, including the 125 training patches, and the other 604 testing patches locate as far as possible from its nearest

Table I. ΔE_{94} color difference between measurement and calculated values.

		Effective coverage mapping				Improved Yule–Nielsen modified spectral Neugebauer model[11]			
ΔE_{94}		Max	Mean	>3	>4	Max	Mean	>3	>4
		Without using *n*-factor				$n = 2.0$			
AM600 dpi-100 lpi Group No. 1	Special (729)	4.94	1.09	30	5	6.84	1.62	77	29
	Random (519)	4.74	1.59	35	6	6.17	2.01	93	30
	All (1248)	4.94	1.30	65	11	6.84	1.78	170	59
	1-2 colors (244)	3.19	0.71	1	0	3.48	1.12	3	0
	3 colors (1004)	4.94	1.44	64	11	6.84	1.94	167	59
						$n = 2.2$			
AM300 dpi-100 lpi Group No. 2	Special (729)	4.48	0.98	18	3	5.87	1.51	64	14
	Random (519)	4.91	1.59	36	8	5.96	1.75	43	9
	All (1248)	4.91	1.23	54	11	5.96	1.61	107	23
	1-2 colors (244)	2.97	0.67	0	0	3.82	1.14	2	0
	3 colors (1004)	4.91	1.37	54	11	5.96	1.73	105	23
						$n = 2.0$			
AM600 dpi-100 lpi Group No. 3 Samples are in different order from group No. 1	Special (729)	4.91	1.09	19	2	7.48	1.91	105	34
	Random (519)	4.68	1.52	31	7	5.40	2.04	79	21
	All (1248)	4.91	1.27	50	9	7.48	1.96	184	55
	1-2 colors (244)	3.13	0.76	1	0	4.71	1.31	11	1
	3 colors (1004)	4.91	1.40	49	9	7.48	2.12	173	54
						$n = 2.6$			
FM1st_300 dpi Group No. 4	Special (729)	6.62	1.29	51	15	8.44	1.77	86	28
	Random (519)	6.79	2.13	100	36	6.55	2.15	105	27
	All (1248)	6.79	1.64	151	51	8.44	1.93	191	55
	1-2 colors (244)	6.27	0.89	8	3	5.02	1.29	8	2
	3 colors (1004)	6.79	1.82	143	48	8.44	2.08	183	53

training points in the effective coverage map coordinate system; "Random (519)" refers to those patches with random reference ink coverage values; "1-2 colors (244)" refers to those patches that involve only 1 or 2 inks, they are totally 244, among which 61 are training patches. They are used to check the performance of the 2D effective coverage grids; "3 colors (1004)" refers to patches involving 3 inks, they are totally 1004; "All (1248)" refers to all 1248 patches. In Table I, besides the average and maximum ΔE_{94} color differences we also show the number of patches for which the ΔE_{94} color differences exceed 3 and 4.

By looking at the results for print group No.1 (AM_600 dpi_100 lpi), we notice that the average ΔE_{94} color difference for all the patches is 1.30 and the maximum ΔE_{94} color difference is 4.94 for the proposed model. The Yule–Nielsen modified spectral Neugebauer model gives 1.78 and 6.84 for average and maximum ΔE_{94} color difference, respectively.

The same models are applied to print group No. 3, which is also printed using AM_600 dpi_100 lpi, but the color samples are put in different order compared to group No. 1. The results presented in Table I for group No. 3 are quite close to that for group No. 1 for our model. For the Yule–Nielsen modified spectral Neugebauer model, the results become worse.

It should be mentioned that in team "1-2 colors (244)" for print group No. 1, the patch which gives the maximum error is (1, 0, 0.63); in team "1-2 colors (244)" for print group No. 2, the patch which gives the maximum error is (0, 0.5, 0.63); in team "1-2 colors (244)" for print group No. 3, the patch which gives the maximum error is (0.63, 0, 0.38) and in team "1-2 colors (244)" for print group No. 4, it is the patch (0, 0.5, 0.63) which gives the maximum error, i.e., 6.27. There is a common reference coverage value: 0.63. It is possible that the test printer is not stable when producing patches around 63% halftone ink. The prediction is affected by the property of the printer, paper, and spectrophotometer that are used. In part of our future work, the performance of our model predicting the color of testing patches with reference coverage values around 63% and 88% will be checked by using other printers or applying different interpolation methods.

The difference between the effective coverage and the reference coverage in FM1st_300 dpi print is found to be generally larger than that for AM print. The dot gain for the inks in FM1st print seems more complicated and is frail to be disturbed during printing, which might be the reason why the ΔE_{94} color difference for FM1st_300 dpi print for both models are worse than AM print.

Print using AM_300 dpi_100 lpi has bigger halftone dots than the print using AM_600 dpi_100 lpi. The results for print group No. 2 (AM_300 dpi_100 lpi) are close to that for groups No. 1 and No. 3 but with smaller maximum error for "1-2 colors (244)". It shows that our model works with no significant difference for AM prints with different screen frequencies. It is necessary to recall that there are only 44 samples used as training in the improved Yule–Nielsen modified spectral Neugebauer model. In our future work, we will try to reduce the number of the training patches by, for example, using different reference coverage combination while keeping a satisfying ΔE_{94} color difference between the predicted and the measured data. This might require modifications of our proposed model.

The above results show that the effective coverage map, which finds the effective coverage of the primary inks using CIEXYZ, respectively, works well in color prediction for prints using AM600 dpi, FM1st300 dpi halftoning. The presented map is simple and running fast. The whole mapping procedure only takes a few seconds.

ACKNOWLEDGMENTS

Appreciation should be delivered to Professor Roger D. Hersch for his useful feedbacks to our questions and for sharing the link http://lsp.epfl.ch/page34136.html with us. The authors are also grateful to Peripheral Systems Laboratory (EPFL), the above link, for offering us the package of their improved Yule–Nielsen modified spectral Neugebauer model.

REFERENCES

[1] D. Wyble and R. Berns, "A critical review of spectral models applied to binary color printing," J. Color Res. Appl. **25**, 4 (2000).
[2] A. Murray, "Monochrome reproduction in photoengraving," J. Franklin Inst. **221**, 721 (1936).
[3] H. Neugebauer, "Neugebauer memorial seminar on color reproduction," Proc. SPIE **1184**, 194 (1937).
[4] M. Namedanian and S. Gooran, "Characterization of total dot gain by microscopic image analysis," J. Imaging Sci. Technol. **55**, 040501 (2011).
[5] F. R. Ruckdeschel and O. G. Hauser, "Yule–Nielsen effect on printing: A physical analysis," Appl. Opt. **17**, 3376 (1978).
[6] L. Yang, S. Gooran, and B. Kruse, "Simulation of optical dot gain in multi-chromatic tone reproduction," J. Imaging Sci. Technol. **45**, 198 (2001).
[7] S. Gustavason, "Dot gain in color halftones," Dissertation No. 492 (Department of Electrical Engineering, Linkoping University, Sweden, 1997).
[8] F. R. Clapper and J. A. C. Yule, "The effect of multiple internal reflections on the densities of halftone prints on paper," J. Opt. Soc. Am. **43**, 600 (1953).
[9] P. Emmel and R. D. Hersch, "A model for color prediction of halftoned samples incorporating light scattering and ink spreading," *Proc. IS&T/SID's 7th Color and Imaging Conference, Color Science, Systems and Applications* (IS&T, Springfield, VA, 1999), pp. 173–181.
[10] J. A. S. Viggiano, "Modeling the color of multi-colored halftones," *Proc. TAGA Conference* (TAGA, Sewickley, PA, 1990), pp. 44–62.
[11] R. D. Hersch and F. Crété, "Improving the Yule-Nielsen modified spectral Neugebauer model by dot surface coverages depending on the ink superposition conditions," Proc. SPIE **5667**, 434 (2005).
[12] R. Rossier and R. D. Hersch, "Introducing ink spreading within the cellular Yule-Nielsen modified Neugebauer model," *Proc. IS&T/SID's 18th Color and Imaging Conference* (IS&T, Springfield, VA, 2010), pp. 295–300.
[13] R. Balasubramanian, "Optimization of the spectral Neugebauer model for print characterization," J. Electron. Imaging **8**, 156 (1999).
[14] S. Gooran, M. Namedanian, and H. Hedman, "A new approach to calculate color values of halftone prints," IARIGAI 36th Research Conference (Advances in Printing and Media Technology, Sweden, 2009).
[15] Y. Qu and S. Gooran, "A simple color prediction model based on multiple dot gain curves," Proc. SPIE **7866**, 786615 (2011).
[16] S. Gooran, "Dependent color halftoning, better quality with less ink," J. Imaging Sci. Technol. **48**, 354 (2004).